w1. Cover Page

Department of Energy
Energy Efficiency & Renewable Energy
Golden Field Office

DOE Grant No.: DE-EE0005316

Project Title:
Single-Crystalline InGaAs/InP Dense Micro-Pillar Forest on Poly-Silicon Substrates for Low-Cost High-Efficiency Solar Cells

Technical Point of Contact/Principal Investigator:

Constance Chang-Hasnain
Electrical Engineering and Computer Sciences
502 Cory Hall #1774
University of California
Berkeley CA 94720-1774
(510) 642-4315; (510) 643-1878 FAX
cch@eecs.berkeley.edu

Submission Date: May 3, 2015

DUNS Number: 124726725

Recipient Organization/Administrative Point of Contact:

The Regents of the University of California
Ms. Patricia Gates
Sponsored Projects Office
2150 Shattuck Ave. Ste. 313
University of California, Berkeley
Berkeley CA 94704-5940
(510) 642-8109; (510) 642-8236
pgates@berkeley.edu

Grant Start/End Dates: 09/01/2011-12/31/2015
Reporting Period End Date: 3/31/15
Report Frequency: Quarterly
Signature of Submitting Official:

2. Accomplishments:

2.1 Major goals of the project

The ultimate goal of this project is to develop a photovoltaic system high conversion efficiency (>20%) using high quality III-V compound-based three-dimensional micro-structures on silicon and poly-silicon. Such a PV-system could be of very low cost due to minimum usages of III-V materials. This project will address the barriers that currently hamper the performance of solar cells based on three-dimensional micro-structures.

To accomplish this goal the project is divided into 4 tasks, each dealing with a different aspect of the project: **materials quality, micropillar growth control, light management, and pillar based solar cells.**

Materials Quality: the internal quantum efficiency (IQE) - by which is meant here the internal fluorescence yield - of the micro-pillars has to be increased. We aim at achieving an IQE of 45% by the end of the first year. By the end of the second year there will be a go-no-go milestone of 65% IQE. By the end of year 3 and 4 we aim to achieve 75% and 90% IQE, respectively.

Micropillar growth control: dense forests of micropillars with high fill ratios need to be grown. Pillars within forests should show minimum variations in size. We aim at achieving fill ratios of 2%, 10%, >15%, >20% in years 1, 2, 3, and 4, respectively. Variations in dimension should be minimized by site-controlled growth of pillars. By the end of year 1 we will aim at achieving site-controlled growth with > 15% yield. By end of year 2 the variation of critical pillar dimensions should be less than 25%.

Light management: high light absorption in the spectral range of the sun has been to be demonstrated for the micropillar forests. By the end of year 1 we will employ FDTD simulation techniques to demonstrate that pillar forests with fill ratios <20% can achieve 99% light absorption. By end of year 2 our original goal was to demonstrate >85% absorption. By end of year 3 > 90% absorption should be demonstrated.

Pillar based solar cells: devices will be studied to explore ways to achieve high open-circuit voltages which will lead to high efficiency micropillar-based solar cells. We will start on single pillar devices and the findings in these studies should pave the way for devices based on forests/ arrays of pillars. By the end of the second year we aim to demonstrate a single pillar device with an open-circuit voltage of 0.7 V, as well as a pillar-forest based device with 8% conversion efficiency. By the end of year 3 these numbers should be improved to 0.9 V open-circuit voltage for single pillar devices and >15% efficiency for forest/array-based devices. We will aim to realize a device with 20% efficiency by the end of the project period.

2.2 Accomplishments under these goals

In the previous reports we showed that some of the outlined goals for the third year project have been already achieved. Namely, the I-V measurements showed that the IQE (i.e. ratio between extracted electrons and adsorbed photons in pillar) of InP single pillar based solar cell device equals ~ 75%. The pillar uniformity studies showed that variation in critical dimension for the pillars is <12% based on SEM studies and <23% based on contactless IV (CIV) measurements. Both experimental and simulated results for light absorption have shown that grown pillars can efficiently adsorb the light, i.e. simulations yielded in 95% light absorption for wavelength of 400-900 nm for a tapered pillar array with volume fill factor of 16%, and experiments showed 92% of light absorption from 300 nm to 900 nm.

In December 2013 the MOCVD growth started to show a poor quality of InP pillars with a very low density of the pillars on Si wafers. A search for a potential problem in growth, variation of growth conditions and order of new MOCVD parts were the main challenges for several months. This lead to repair of MOCVD machine in June 2014 and establishing new growth conditions for the pillars in the period of June-September 2014. After finding appropriate and reproducible growth conditions for InP pillars, we have focused on the fabrication of InP pillar based solar cell devices.

2.2.1. Characteristics of the p+ - InP devices

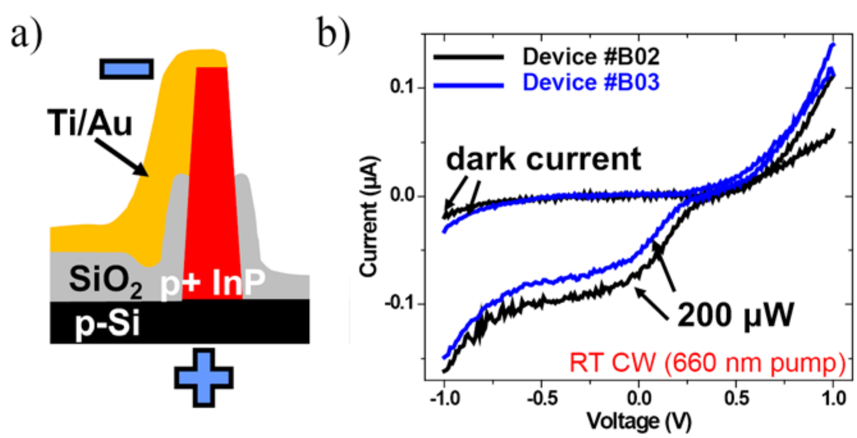

Fig. 1. a) Schematic model of the single p^+-doped InP pillar device grown on p-doped silicon substrate with Ti/Au contacts deposited on one side of the pillar. b) IV characteristics of two devices (labeled as #B02 and #B03) fabricated on the same sample recorded at room temperature (RT). Continuous wave (CW) laser at 660 nm was used as an optical pump. Dark current and photocurrent at 200 μW pump are represented.

In our previous reports it has been shown that the solar cell devices based on InP pillars suffer from high resistance and low p-doping concentration, which cannot be improved with existing

MOCVD machine, due to limitations on in-situ Zn incorporation during growth. In order to analyze a reason of the high resistance in InP devices, the highly p^+-doped InP pillars were grown on the p-doped Si substrate (here and later, p^+-doped InP pillars correspond to the maximum p-doping achieved by MOCVD). SiO_2 mask was used in order to separate bottom of the pillars from the metallic contact, as shown in schematic Fig. 1 a). Ti and Au metallic contacts were deposited by angle electron-beam evaporation method, where only the pillars were contacted by metallic contacts only on one side.

After fabrication, the pillars were exposed to the continuous wave (CW) laser operated at 660nm, which was used as an optical pump source. IV characteristics of the fabricated devices were recorded under no irradiation (dark current) and CW laser irradiation corresponded to 200 μW. The IV characteristics of two devices fabricate on the same sample are shown in Fig. 1 b) in sweeping bias of -1 V to +1 V.

A Schottky contact is built on the interface between the InP pillars and Ti/Au metallic contact. Both devices in Fig. 1 b) showed open circuit voltage, V_{oc}, of ~ 0.35 V. A high bulk series resistance is revealed at higher (close to 1 V) bias and estimated to be ~ 2-3 $M\Omega$ for device #B02 and #B03, respectively. Estimated p-doping concentration of the studied InP pillars is in the order of 10^{15} cm^{-3}, which is significantly low from the desired value of ~ 10^{17}- 10^{18} cm^{-3}. Hence, the high resistance observed in the InP pillars with n-p and n-i-p junctions (shown in the previous reports) is mainly originates from the very high InP bulk series resistance due to the low p-doping concentration of the pillars.

Moreover, the I-V curves recorded under 200 μW irradiation have a very pronounced S-like shape. This S-shape has not been observed for any previously fabricated devices and seems to be characteristic for the p-core InP device. The origin of the shape is due to the low p-doping, which leads to minority carrier recombination at the silicon-InP interface at the root of the pillar.

Since p-doping of InP pillars cannot be improved in-situ by MOCVD, this leads us to a new approach of InP p-doping using ex-situ method by closed-space sublimation chamber, which will be further discussed. Moreover, we worked on redesign of the InP based solar cell devices in order to improve their efficiency and avoid high series resistance and current leakage.

2.2.2. Device structures

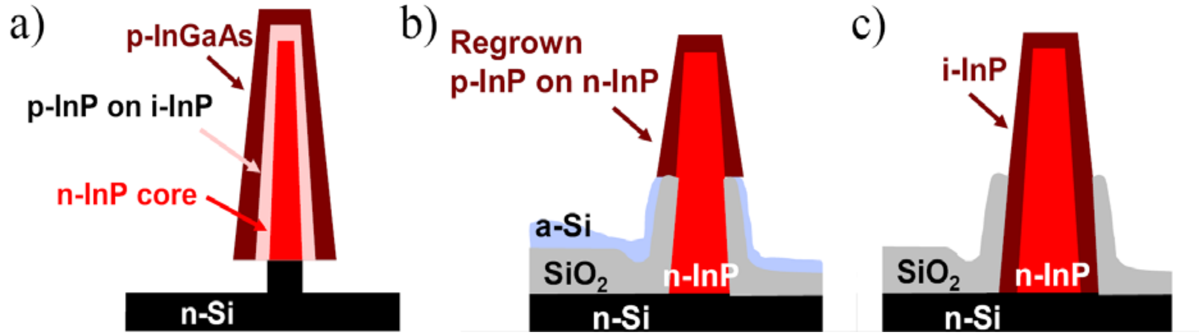

Fig. 2. Schematic representation of the fabricated InP solar cell devices: a) *undercut* of the structure n-InP core / i-InP shell/ p-InP shell / p-InGaAs shell, b) *regrowth* process — n-InP core / regrown p-InP on n-InP shell, c) structure for *ex-situ Zn-diffusion* — n-InP core / i-InP shell.

We have work on the redesign of the InP pillar based devices in order to eliminate two of the biggest challenging we were facing in the previous work, namely

- current leakage
- high resistance

In order to avoid the current leakage, a new undercut etching process has been proposed. Undercut implies a silicon substrate dry etching, where the silicon is etched till the core of the pillar, as sketched in Fig. 2 a). As a result, a shunt path from p-InP shell into n-Si is eliminated preventing thus significantly reducing the current leakage. Undercut etching is an alternative approach to the previously reported regrowth process.

As shown in Fig. 2 b), the regrowth takes place on the upper part of the pillar, where the n-InP core is grown during initial growth and the bottom part of the pillar is isolated by PECVD deposited SiO_2 and amorphous Si (a-Si) layer. In order to make the interface between the initial growth and the regrown layer smoother and defect free, a thin n-InP layer is deposited as a first step of the regrowth. Afterwards, a p-InP outer shell layer is regrown. Similar to the undercut process, the regrowth prevents the shunt current between the p-InP and n-Si substrate.

We also propose two designs of the InP device structures to avoid high resistance discussed in section 2.2.1. First approach is to passivate the undercut structure shown in Fig. 2 a) with a thin p-InGaAs outer shell. The 5-10 nm thick p-InGaAs cap layer is known to significantly improve contact resistance between InP and metallic contacts. Second approach is to improve p-doping of the InP shell of the pillar by performing ex-situ Zn diffusion. For this, the n-InP core should be overgrown with the i-InP outer shell which will be exposure for the Zn diffusion process. Again, in order to prevent current leakage from the outer shell to the substrate, a SiO_2 mask is used for isolation, as sketched in Fig. 2 c).

Each of the proposed devices have been fabricated and their electrical characteristics have been measured and compared to each other as well as previous reported values. The up-to-date results for each of the device shown in Fig. 2 are discussed below in details.

2.2.2.1. Device with undercut

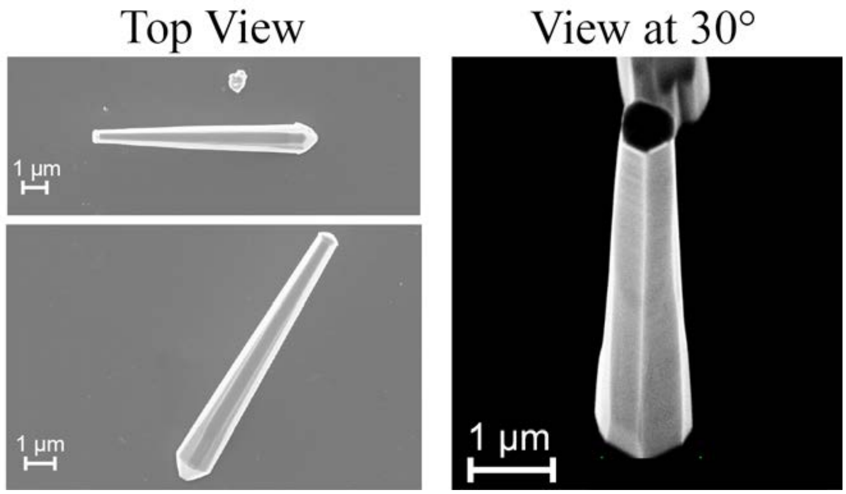

Fig. 3. Top and side view (tilt at 30°) SEM images of the n-InP core / i-InP shell/ p-InP shell / p-InGaAs shell structure before undercut.

For the undercut device, the InP pillar was grown by MOCVD on the n-Si substrate. The InP pillar has a n-InP core covered by i-InP shell, which is overgrown with p-InP shell. Additionally, the p-InP shell of the pillar was covered with 5 nm p-InGaAs cap layer which is designed to improve contact resistance between the pillar and metallic contacts. The whole InP pillar structure was grown in one growth run, so the sample was not exposed to ambient air between the growths of different layers.

The top and side view SEM images of the grown InP pillars in Fig. 3 show very good crystal quality of the pillars with well pronounced and defect free hexagonal facets of the pillars. The 'Technics C Plasma Etching System' was used to perform an undercut of the represented pillars. Different plasma etching parameters and gases were tested prior the appropriate etching recipe was found. The sulfur hexafluoride (SF_6) gas mixed with an oxygen gas (O_2) at the flow rate of 60sccm and plasma power of 50 W lead to the homogeneous and reproducible etching of the Si substrate.

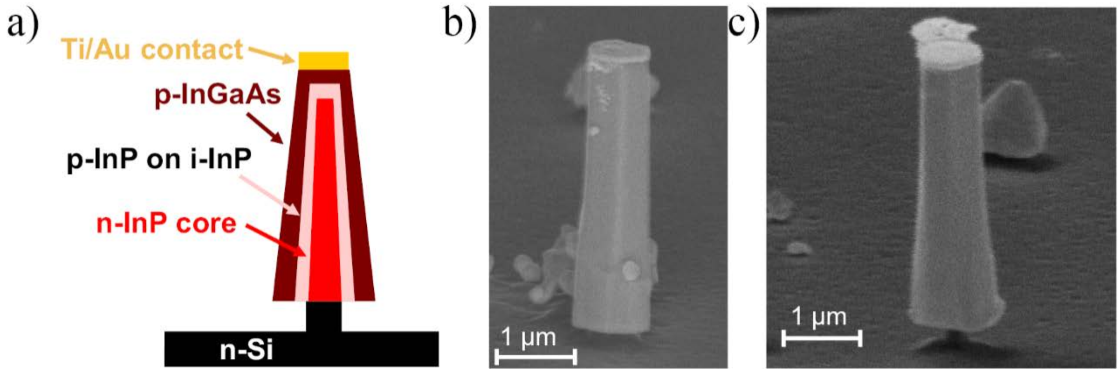

Fig. 4. a) Schematic model of the n-InP core / i-InP shell/ p-InP shell / p-InGaAs shell structure. SEM images of that undercut structure after etching in SF6/O2 plasma for b) 30 sec (tilt view at 75°) and c) 45 sec (tilt view at 65°).

SEM images of the undercut structure are shown in Fig. 4 b) and c) for the plasma etching time of 30 sec and 45 sec, respectively. Upon the etching, n-Si substrate was etched under the pillar by 200-250 nm for 30 sec etching time and by 300-350 nm for 45 sec etching time if taking into account only one side of the pillar. The remaining Si pedestal has a diameter of 600-650 nm in case of 30 sec etch but only 200-250 nm diameter for 45 sec etch time. Surprisingly, InP pillars remained standing despite a very narrow diameter of the Si pedestal, as shown in Fig. 4 c). This indicates a very robust structure of the pillars.

Estimated radius of the n-InP core is 200nm and radius of th i-InP and p-InP shell are ~130nm and ~200nm respectively, making the minimum size of the Si undercut for preventing shunt current from p-InP shell into substrate of 200nm in radius. This conditions are satisfied in case of both etching runs discussed above.

However, fabrication of the devices with 200-250nm pedestal resulted in falling of the InP pillars, so no devices could be tested. Fabrication of the second sample is currently under processing. First results showed that developed undercut etching process results in low dark current of 10pA and 10^4 fold reduction of current leakage.

2.2.2.2. Regrown device

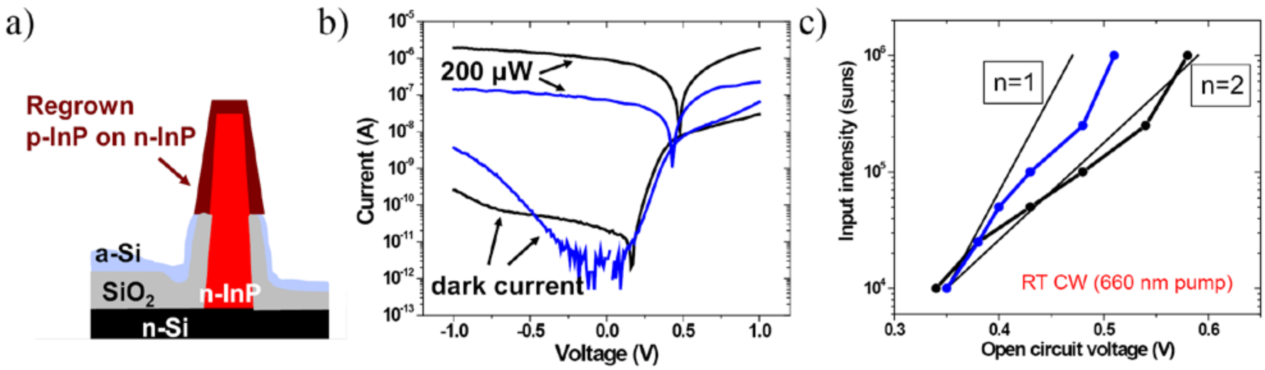

Fig. 5. a) Schematic model of the regrown structure: n-InP core / regrown p-InP on n-InP shell, b) I-V characteristics of the two InP based devices (blue and black curves) grown on same sample recorded under no irradiation (dark current) and CW laser irradiation corresponded to 200 µW. c) Calculated ideality factors for these two devices along with the lines referred to n=1 and n=2 as guide to the eye.

The InP device based on the regrowth process had a structure depicted in Fig. 5 a). The n-InP core has been initially grown on n-Si substrate. Afterwards, the sample was exposure to ambient air and layers of SiO_2/a-Si/SiO_2 have been deposited by PECVD. After several steps of etching, the top part of the InP pillar was exposed to air, while the bottom part was isolated by SiO_2/a-Si layer. The regrowth was performed on this structure.

First step of the regrowth was a growth of a thin n-InP layer for better interface quality between the initially grown and regrown layers. Afterwards, the gases in MOCVD were switched that a p-InP layer could be grown as an outer shell.

Similar to the above discussed p^+-InP devices, the metallic Ti/Au contacts were deposited by the angle electron beam metal evaporator covering one side of the InP pillars. The I-V characteristics of two devices are shown in Fig. 5 b) for dark current and photocurrent under laser irradiation of 200µW. Both devices (blue and dark lines) are from the same sample and fabrication run showing very similar behavior and reproducibly of the device characteristics.

No S-like shape can be observed in the I-V curves, as it was highly pronounced in the I-V curves for the p^+-InP devices. Hence, the S-like shape can be eliminated for p-n-junction based InP pillars and is a characteristic of only p^+-InP pillars grown on p-Si substrate. The input intensity versus open circuit voltage for both devices are represented in Fig. 5 c) along with the lines for ideality factors n=1 and n=2. The open circuit voltage for both devices have value of $V_{oc} \approx 0.5V$, which is significantly better than the p^+-InP devices described above and comparable to the previously reported results.

A large series resistance is still observed at higher bias indicating a low p-doping concentration of the grown InP pillars. The way to improve the p-doping concentration is discussed in the next section, where an ex-situ method of Zn diffusion by using closed-space sublimation chamber is applied.

2.2.3. P-doping of InP by Zn diffusion

2.2.3.1. Zn diffusion by closed-space sublimation (CSS)

Efficient p-doping in InP nanopillars has been challenging due to difficulty in incorporation of acceptor atoms. 4 point probe measurements show poor p-doping of ~$10^{15}/cm^3$ in pillars grown with in-situ p-doping using a metal organic diethylzinc (DeZn) source. In order to achieve p-n junction devices, p-doping needs to be improved significantly; for this - ex-situ doping techniques were explored. Zn diffusion in a closed space sublimation (CSS) furnace was performed in Prof. Ali Javey's laboratory. Zn diffusion in a CSS furnace (shown in Fig. 6 a)) has shown promising results on planar InP films. During CSS, the samples are placed in a tube furnace, with solid Zn_3P_2 powder used as the source. The chamber pressure is pumped down to ~250 mT. The substrate and Zn source are about ~2 cm apart, with the source temperature set at 520°C, while the sample temperature is set at 420°C. The dissociation of the Zn_3P_2 source produces phosphorus and maintains a phosphorus overpressure. Figure 6 b) shows the results of a drive level capacitance profiling measurement on InP films with Zn diffusion performed for 1 hr, where an acceptor doping of ~$10^{17}/cm^3$ and the depth of doping of ~100 nm are measured.

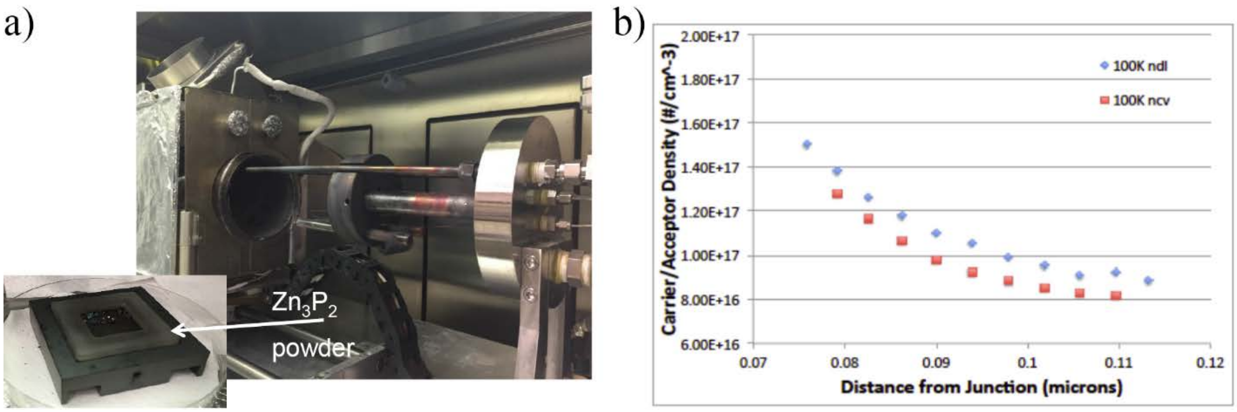

Fig. 6. a) Closed-space sublimation furnace, inset shows Zn_3P_2 source powder. b) Drive level capacitance profiling on ITO/TiO2/p-InP/Mo planar devices.

This confirms that the pillars can withstand the CSS doping conditions. The nanopillars sample was kept under similar conditions (T_{sub}= 390°C, T_{source}=490°C) for 1 hour. SEM image of the same pillars before and after this process reveals that the nanopillars do not undergo any degradation or surface reconstruction for up to 1 hour in the furnace.

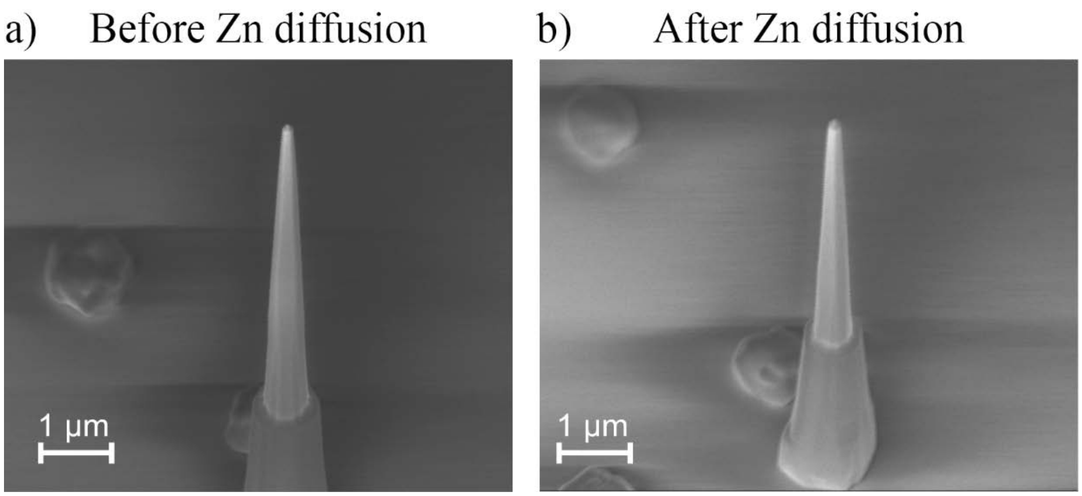

Fig. 7. Scanning electron micrograph of a nanopillar a) before and b) after 1 hour in the CSS furnace.

2.2.3.2. Ensemble device fabrication and characterization

The activation of diffused dopant species (Zn) is measured by fabrication of electrical p-n junction devices. The structure used to test the doping through Zn diffusion consists of a MOCVD grown Te-doped n-core, followed by a 130 nm intrinsic InP shell, as shown below in Fig. 8.

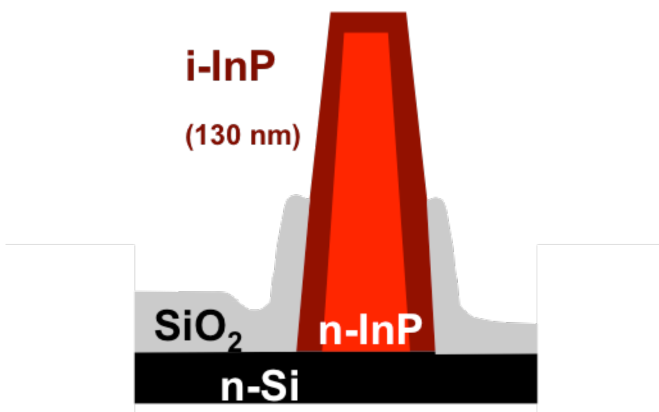

Fig. 8. Schematic of the nanopillar structure used to fabricate ensemble devices.

The fabrication process for electrical devices is outlined below in Fig. 9. The nanopillar samples grown on n-doped Si substrates were first covered with a conformal 200 nm layer of plasma enhanced chemical vapor deposited (PECVD) silicon dioxide. The oxide provides electrical isolation between the top and bottom contacts. The oxide is then partially etched down using a combination of photolithography, dry etching of the photoresist, followed by the wet etching of oxide.

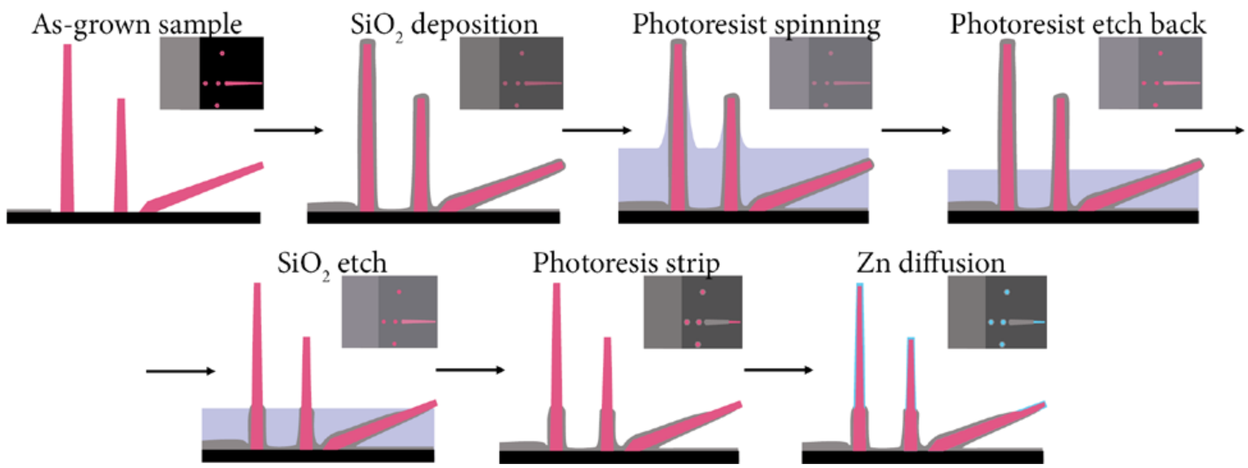

Fig. 9. Fabrication process flow

After the tops of the nanopillars are exposed, the sample is loaded in the CSS chamber for Zn diffusion. Zn diffusion through the nanopillar surface creates a radial p-n junction. In order to fabricate diodes (steps shown in Fig. 10), the p-doped shell is contacted using Zn/Au, which is a known ohmic contact to p-InP. The contact deposition takes place via thermal evaporation at a 45-degree angle. After liftoff, the p-contact is annealed at 250°C for 2 minutes to form a Zn-Au alloy, which reduces the contact resistance. The degenerately n-doped Si is used a backside n-contact.

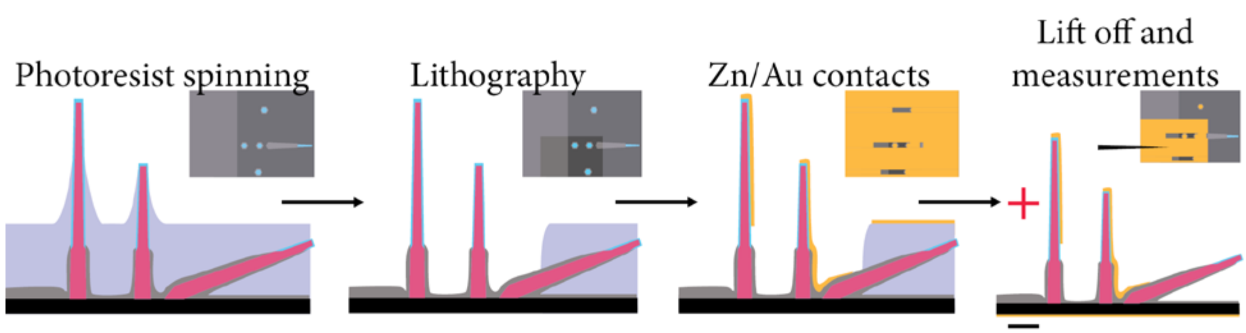

Fig. 10. Fabrication process flow

An SEM image of a fabricated nanopillar device after Zn/Au liftoff is shown in Fig. 11 a). The devices show diode-like behavior with turn-on at ~0.5 V and diode-ideality factor n ~ 2. The ensemble devices contain 2-3 nanopillars per pad and show forward resistance 3-7 KΩ. The devices show a relatively large reverse current, which may be attributed to a leakage path created by the diffusion of the Zn atoms in the region protected by the oxide mask. To circumvent this problem, CSS doping is being investigated in regrown nanopillars.

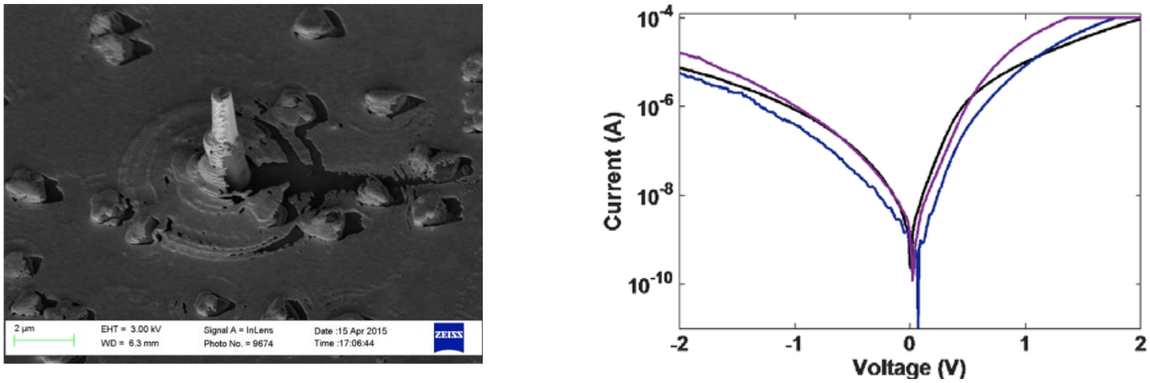

Fig. 11. (a) SEM image of nanopillar with Zn/Au metal contact, (b) room-temperature I-V characteristics for different ensemble devices.

2.2.3.3. Controlling the depth of the Zn diffusion

In order to control the depth of Zn diffusion doping we vary the diffusion time in the CSS step. A sample with a single InGaAs quantum well inserted in the heterostructure (shown in Fig. 12 a)) was used to determine the diffusion depth of the Zn dopants. Based on the shift in the quantum well emission, we estimate the depth of Zn diffusion. The photoluminescence from the quantum well shows a red shift if Zn diffuses into the quantum well active region. For 1 hr of CSS doping, the quantum well emission shifts more than 200 nm, which is beyond the detection limit for our CCD. PL spectra for QW before Zn diffusion and after 10 mins, 20 mins of Zn diffusion are shown in Fig. 12 b). Based on this, we estimate 10 minutes of CSS doping is suitable to dope ~130 nm of InP without degrading the optical properties of the active region.

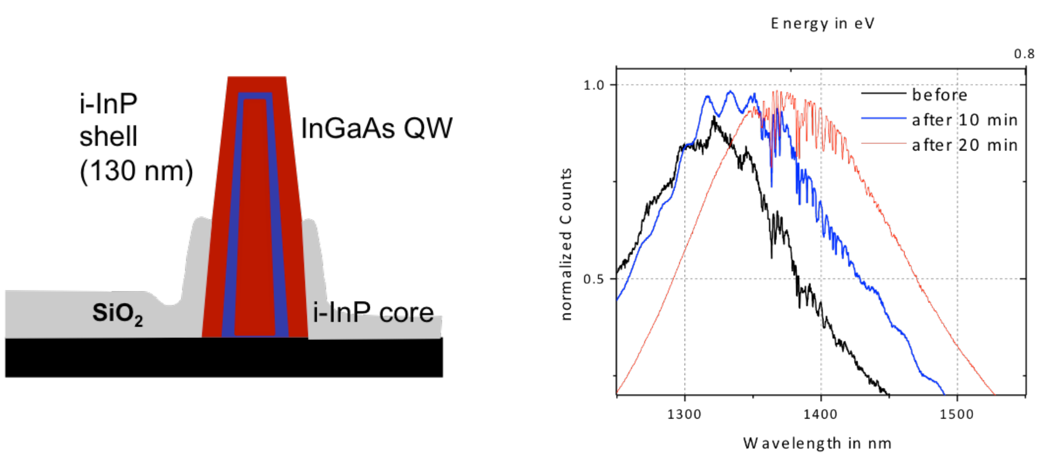

Fig. 12 a) Schematic of QW heterostructure to study depth of Zn diffusion, b) PL spectra measured from nanopillar before and after Zn diffusion.

2.2.4. Growth improvements

2.2.4.1. High density of pillars

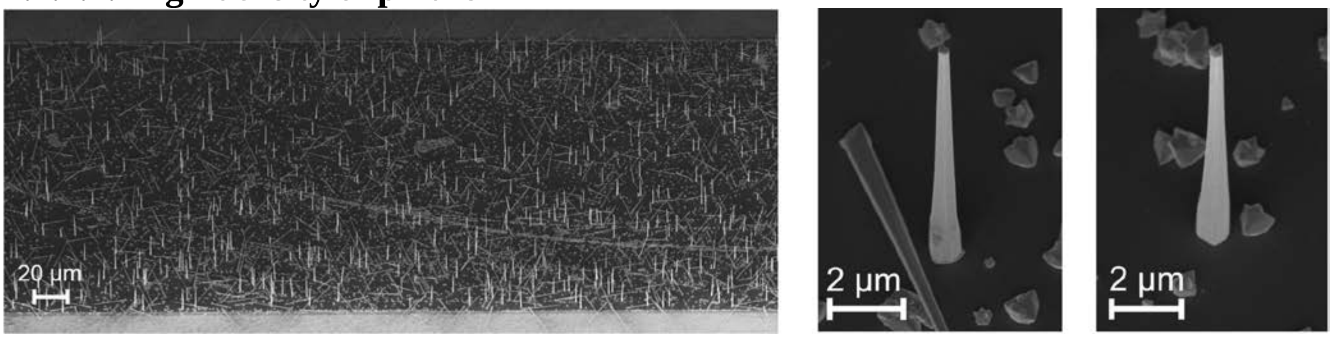

Fig. 13. SEM images of i-InP pillars grown on i-Si-substrate at different magnifications.

After repairing MOCVD machine in June 2014 and finding appropriate growth parameters, which result in good crystal and optical quality of the InP pillars, we continued the work on improving density of the InP pillars. One of the main challenges were improve density of the pillars across entire 2-inch Si wafer. A growth of the pillars in the center of the wafer was often lacking of any pillar grown, while pillars have good density close to the edges of the wafer.

One of our last achievement is a significant improvement in the density of i-InP pillars across the entire 2-inch wafer. The high density growth can be easily reproduced, the pillars have good crystal quality as shown in Fig. 13, and their shape and length is similar to each other across the wafer. The growth of the pillars also occurs in the center of the wafer, although with a lower density than next to the edges. The pillars in the center of the wafer have shorter length (3-6 μm) but good crystal quality, comparable to the one next to the edges. The difference in the pillar length and density across entire 2-inch wafer can be explained due to different gas flux fluctuation and temperature gradient on the wafer.

2.2.4.2. Regrowth of InP pillars

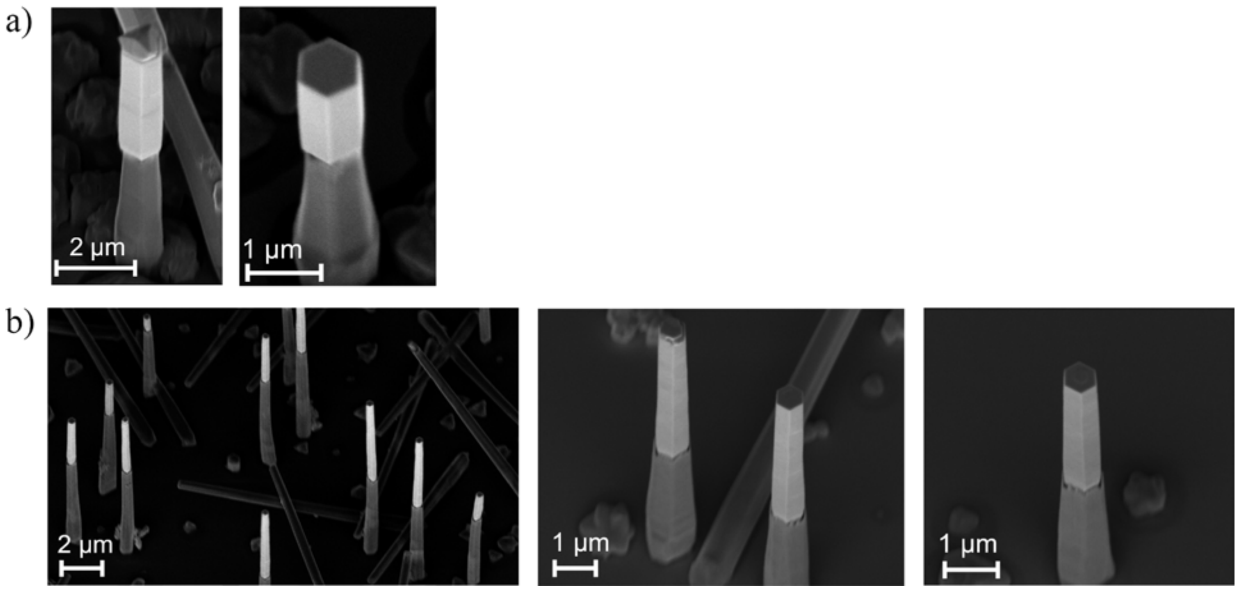

Fig. 14. First successful regrowth after MOCVD failure. SEM images of i-InP pillars from a) Sample 1 and b) Sample 2

After fixing the MOCVD machine the previous year, an old recipe for the regrowth process was not reproducible and we worked on finding regrowth conditions as well as new substrate preparation conditions. The main challenge is to obtain a homogeneously covered regrown layer on top of the initial grown pillar with no or minimum defects.

After many attempts the regrowth process was successfully obtained on Sample 1 (Fig. 14 a) and reproduced on Sample 2 (Fig. 14 b). SEM shows that all pillars have uniformly formed regrown layer. Sample 1 and 2 are i-InP core pillars grown on i-Si substrate with i-InP regrown outer shell. The further steps are to decrease defects density in the regrown layer and to perform a regrowth on n-InP core pillars for further fabrication of the devices.

2.3 Training and professional development provided by project

The activities described above required operation of metal-organic chemical vapor deposition (MOCVD) equipment for materials synthesis, as well as scanning electron microscopy (SEM), transmission electron microscopy (TEM), and photoluminescence spectroscopy for materials characterization. Therefore, these studies provided extensive technical training to graduate students and post-doctoral researchers. Another dimension of training is project management; carrying out the concerted activities described above required detailed coordination and planning of the actions by involved personnel.

Since December 2013 three students have obtained their PhD degrees: two students in December 2013, one student in July 2014. Among them, one student accomplished his work as a postdoctoral researcher in September 2014. Another graduate student finished her 2-years PhD-exchange program at UC Berkeley in July 2014.

2.4 Planning for next reporting period to accomplish goals and objectives

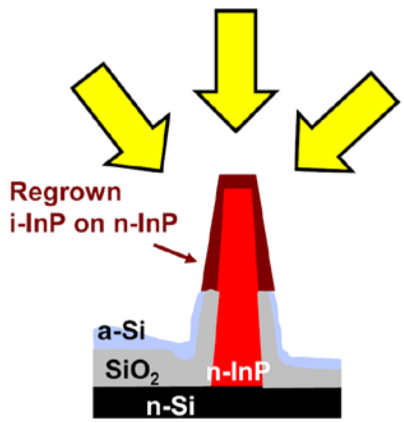

Fig. 15. Schematics showing Zn diffusion process for the regrown device n-InP core / regrown i-InP on n-InP shell

We will intensify our efforts to improve the device performance. Currently, our device performance is limited by low p-doping concentrations. We will continue our investigation of improving p-doping of InP by Zn diffusion using CSS chamber and apply this ex-situ doping model to the regrown device shown in Fig. 15. In this model the n-InP pillar will be grown as initial growth and overgrown with i-InP on n-InP layer during the regrown process. The outer i-InP shell will be exposed to CSS for Zn diffusion. Moreover, to improve metallic contacts, we anneal the Zn/Au contacts at different temperatures by using rapid thermal annealing. We will also experiment with InGaAs-cap layer pillars.

We continue our work on undercut InP device and compare their optical and electrical quality to the regrown device with ex-situ doped outer shell. Additionally, we resume the work on site control growth in order to obtain ensemble devices with high density of InP pillars.

3. Products

Since the report from April 2014 we have produced several publishable results that have been or will be presented in peer-reviewed journals and conferences:

[1] T. D. Tran, H. Sun, K.W. Ng, F. Ren, K. Li, F. Lu, E. Yablonovitch, and C. J. Chang-Hasnain, "High Brightness InP Micropillars Grown on Silicon with Fermi Level Splitting Larger than 1 eV", Nano Letters **2014**, *14* (6), pp. 3235-3240

[2] R. Chen, K. W. Ng, W. Ko, D. Parekh, F. Lu, T. D. Tran, K. Li and C. J. Chang-Hasnain "Nanophotonic integrated circuits from nanoresonators grown on silicon", Nature Communications **2014**, *5*, pp. 4325

[3] H. Sun, F. Ren, K. W. Ng, T. D. Tran, K. Li and C. J. Chang-Hasnain, "Nanopillar Lasers Directly Grown on Silicon with Heterostructure Surface Passivation", ACS Nano **2014**, *8* (7), pp. 6833-6839

[4] K. W. Ng, W. S. Ko, F. Lu and C. J. Chang-Hasnain, "Metastable Growth of Pure Wurtzite InGaAs Microstructures", Nano Letters, **2014**, *14*, pp. 4757−4762

[5] H. Sun, F. Ren, T. D. Tran, K. W. Ng, K. Li, W. Ko, I. Bhattacharya and C. J. Chang-Hasnain, poster presentation "High Voc Solar Absorbers for High Efficiency, Spectral Splitting Solar Cells", BAPVC Bi-Annual Meeting, October 6-7, 2014, Berkeley

Following papers are under preparation for publication in peer- reviewed journals:

[1] W. S. Ko, T. Tran, I. Bhattacharya, K. W. Ng, H. Sun, and C. J. Chang-Hasnain, "Illumination angle insensitive single indium phosphide tapered nanopillar solar cell", submitted to Nano Letters

[2] H. Sun, K. W. Ng, F. Ren, T. Tran, K. Li and C. J. Chang-Hasnain, "First Observation of Composition Ordering in Wurtzite-Phase InGaP Nanoneedle Lasers on Silicon", submitted to Nature Communications

4. Participants & Other Collaborating Organizations:

Name: Constance Chang-Hasnain

Project Role: Principal Investigator

Nearest person month worked: 1

Contribution to Project: provided supervision and scientific direction for the project.

Funding Support (Other than from award): National science Foundation, Defence Advanced Research Projects Agency

Name: Ming Wu

Project Role: Co-Principal Investigator

Nearest person month worked: 0.2

Contribution to Project: providing supervision on optical characterization.

Funding Support (Other than from award): National science Foundation, Defense Advanced Research Projects Agency

Name: Eli Yablonovitch

Project Role: Co-Principal Investigator

Nearest person month worked: 0.2

Contribution to Project: providing supervision on the task of light trapping.

Funding Support (Other than from award): National science Foundation, Defense Advanced Research Projects Agency

Name: Thai Tran

Project Role: Postdoctoral Researcher

Nearest person month worked: 3

Contribution to Project: Device process development for pillar based solar cells

Funding Support (Other than from award): None

Name: Hao Sun

Project Role: Graduate Student

Nearest person month worked: 3

Contribution to Project: Device process development for pillar-based ensemble devices

Funding Support (Other than from award): None

Name: Indrasen Bhattacharya

Project Role: Graduate Student

Nearest person month worked: 3

Contribution to Project: Optical and electrical characterization of pillar material

Funding Support (Other than from award): None

Name: Fanglu Lu

Project Role: Graduate Student

Nearest person month worked: 3

Contribution to Project: Synthesized and characterized micropillar materials.

Funding Support (Other than from award): None

Name: Wai Son Ko

Project Role: Graduate Student

Nearest person month worked: 3

Contribution to Project: Synthesized and characterized micropillar materials.

Funding Support (Other than from award): None

Name: Gregg Scranton

Project Role: Graduate Student

Nearest person month worked: 3

Contribution to Project: Electromagnetic modeling

Funding Support (Other than from award): None

Name: Michael Eggleston

Project Role: Graduate Student

Nearest person month worked: 3

Contribution to Project: Optical characterization of pillar material

Funding Support (Other than from award): None

Name: Seth Fortuna

Project Role: Graduate Student

Nearest person month worked: 3

Contribution to Project: Device process development for devices

Funding Support (Other than from award): None

Name: Daria Skuridina

Project Role: Postdoctoral Researcher

Nearest person month worked: 3

Contribution to Project: Synthesized and characterized micropillar materials.

Funding Support (Other than from award): None

Name: Saniya Deshpande

Project Role: Postdoctoral Researcher

Nearest person month worked: 3

Contribution to Project: Synthesized and characterized micropillar materials.

Funding Support (Other than from award): None

5. Impact

The results presented here suggest that InP micropillar solar cells have the potential of achieving high open-circuit voltages, if size, surface properties, and doping are all optimized. While in this work InP was used it should be in principle possible to achieve similar results with other III-V materials such as GaAs if surfaces can be passivated with epitaxially grown higher bandgap materials. Another key aspect that allowed for the high pillar performance was their micrometer-scale sizes which could be achieved using the core-shell growth mode. To our knowledge there are no reports published in which structures of similar size were synthesized using more common methods like VLS or selective area growth (SAG) which are inherently axial growth modes, i.e. the nanowires predominantly grow in vertical direction with little to no material deposition at on side-facets. But it has been shown that by changing the nanowire growth conditions it is possible to switch from axial growth modes to core-shell. Therefore, the we are optimistic that the performances shown here are not restricted to the pillars presented here, which were grown with a peculiar core-shell method, but that they could also be achieved in structures synthesized via more common nanowire growth methods such as VLS or SAG. These and future results might therefore suggest design rules for achieving high open-circuit voltages in nano-and microstructure based III-V solar cells, and which has been the fundamental limiting challenge for nanowire solar cells. As such structures could be grown on lattice mismatched substrates such as silicon the high costs of III-V substrates, which is the main commercial barrier for III-V photovoltaics, could be mitigated.

Furthermore, from a broader perspective, these results hint at excellent surface properties of InP material, bringing up an old question of whether homostructure III-V solar cells can compete with heterostructures. Using homostructure solar devices would further allow for streamlining the manufacturing process and reduce costs.

6. Changes, Problems --- Nothing to Report

7. Special Reporting Requirements --- Nothing to Report

Award Number: **DE-EE0005316**
Project Title: **Single-Crystalline InGaAs/InP Dense Micro-Pillar Forest on Poly-Silicon Substrates for Low-Cost High-Efficiency Solar Cells**
Recipient: **University of California, Berkeley**
Primary Contact: **Constance Chang-Hasnain**

I. Project Management Plan

	Task	Sub-Task	Point of Contact (POC)	Criteria	Tool/Method of Measurement	Milestone/Go-No Go/Metric	Demonstration	Month 01-48																Task Dates				Milestone or Go/No-Go Dates		Progress Notes
								Q1	Q2	Q3	Q4	Q5	Q6	Q7	Q8	Q9	Q10	Q11	Q12	Q13	Q14	Q15	Q16	Planned		Actual				
																								Start	End	Start	End	Planned	Actual	
Phase I	1	1	C. Chang-Hasnain (510) 642-431	Increase IQE of pillars	MOCVD, Optical Spectroscopy	45% IQE	Document	X	X	X	X													09/30/11	09/30/12	01/01/12	01/01/13	09/30/12	01/01/13	>1 eV fermi-level split demonstrated in n-doped InP
	2	2.1	C. Chang-Hasnain (510) 642-431	Site-controlled pillar forest growth	Lithography, MOCVD, SEM	Volume fill ratio of >2% or 15% yield	Document	X	X	X	X													09/30/11	09/30/12	01/01/12	01/01/13	09/30/12	01/01/13	Growth InP pillars with densities up to 6.6x10^5 pillars per cm^2 which is consistent with 2% fill ratio
		2.2		Pillar uniformity Study	Lithography, MOCVD, SEM, Computer, Optical Spectroscopy	Establish dependence on growth parameters	Document	X	X	X	X													09/30/11	09/30/12	01/01/12	01/01/13	09/30/12	01/01/13	Studying effects of temperature, V/III-ratio, doping on InP pillars
	3	3	C. Chang-Hasnain (510) 642-431	Light management	FDTD Simulation	Optical design that has 99% light absorption with <20% filling ratios	Document	X	X	X	X													09/30/11	09/30/12	01/01/12	01/01/13	09/30/12	01/01/13	Demonstrate randomly oriented pillars with fill ratios
	4	4	C. Chang-Hasnain (510) 642-431	Device Modeling	FDTD, FEM, Device Modeling Tools	Quantitative model of efficiency dependence on size variations	Document	X	X	X	X													09/30/11	09/30/12	01/01/12	01/01/13	09/30/12	01/01/13	Fermi-splitting variability gives a very small value of <2% comparing to average of 1.05V.
Phase II	1	1	C. Chang-Hasnain (510) 642-431	Increase IQE of pillars	MOCVD, Optical Spectroscopy	65% IQE **(go-no-go)**	Document					X	X	X	X									10/01/12	10/01/13	01/02/13	01/01/14	10/01/13	01/01/14	I-V shows IQE (i.e. ratio electrons extracted and photons absorbed) ~75%
	2	2.1	C. Chang-Hasnain (510) 642-431	Site-controlled pillar forest growth	Lithography, MOCVD, SEM	fill ratio>10% (**go-no-go**)	Document					X	X	X	X									10/01/12	10/01/13	01/02/13	01/01/14	10/01/13	01/01/14	Site controlled growth with volume fill ratios larger than 12%
		2.2		Pillar uniformity Study	Lithography, MOCVD, SEM, Computer, Optical Spectroscopy	<25% critcal dimension variation	Document					X	X	X	X									10/01/12	10/01/13	01/02/13	01/01/14	10/01/13	01/01/14	Measure nanopillar uniformity based contactless IV and SEM: <12 % (SEM) <23 % (CIV)
	3	3	C. Chang-Hasnain (510) 642-431	Light management	Reflection, Transmission setup	Experimental demonstration >85% absorption (**go-no-go**)	Document					X	X	X	X									10/01/12	10/01/13	01/02/13	01/01/14	10/01/13	01/01/14	Light absorption of 88% from 300nm-900nm
	4	4.1	C. Chang-Hasnain (510) 642-431	Realize single pillar device	Electron Beam Lithography	>0.7V open-circuit voltage (**go-no-go**)	Document					X	X	X	X									10/01/12	10/01/13	01/02/13	01/01/14	10/01/13	01/01/14	Under 1 sun illumination Voc was measured to be 0.55V at 25 °C, 0.63V at -25 °C, and 0.7V at -100 °C
		4.2	C. Chang-Hasnain (510) 642-431	Fabricate pillar forests devices	Standard Microfabrication Techniques	8% conversion efficiency	Physical Specimen, Document					X	X	X	X									10/01/12	10/01/13	01/02/13	01/01/14	10/01/13	01/01/14	9.6 % for self assembled pillars under 1-sun illumination. 9% for top-down etched pillars under 1-sun illumination
	1	1	C. Chang-Hasnain (510) 642-431	Increase IQE of pillars	MOCVD, Optical Spectroscopy	75% IQE	Document									X	X	X	X					10/02/13	10/01/14	01/02/14	02/01/15	N/A	N/A	I-V shows IQE (i.e. ratio electrons extracted and photons absorbed) ~75%

	Task	Sub-Task	Point of Contact (POC)	Criteria	Tool/Method of Measurement	Milestone/Go-No Go/Metric	Demonstration	Month 01-48																Task Dates				Milestone or Go/No-Go Dates		Progress Notes
								Q1	Q2	Q3	Q4	Q5	Q6	Q7	Q8	Q9	Q10	Q11	Q12	Q13	Q14	Q15	Q16	Planned		Actual				
Phase III	2	2.1	C. Chang-Hasnain (510) 642-431	Site-controlled pillar forest growth	Lithography, MOCVD, SEM	fill ratio>15%	Document									X	X	X	X					10/02/13	10/01/14	01/02/14	02/01/15	N/A	N/A	Site controlled growth with volume fill ratios larger than 12%. Repaired MOCVD tool after critical failure. Optimized growth parameters are found. Currently working on regrowth optimization.
		2.2		Pillar uniformity Study	Lithography, MOCVD, SEM, Computer, Optical Spectroscopy	<15% critcal dimension variation	Document									X	X	X	X					10/02/13	10/01/14	01/02/14	01/01/15	N/A	N/A	Measure nanopillar uniformity based contactless IV and SEM: <12 % (SEM) <23 % (CIV)
	3	3	C. Chang-Hasnain (510) 642-431	Light management	Reflection, Transmission setup	>90% absorption	Document									X	X	X	X					10/02/13	10/01/14	01/02/14	01/01/15	N/A	N/A	Simulation: Light absorption of 95% from 400nm-900nm of tapered pillar array with volume fill factor of 16%. Experiment: Light absorption of 88% from 300nm-900nm
	4	4.1	C. Chang-Hasnain (510) 642-431	Optimize single pillar cell	Electron Beam Lithography	0.9V open-circuit voltage	Document									X	X	X	X					10/02/13	10/01/14	01/02/14	02/01/15	N/A	N/A	19.6 % for single InP pillar solar cell under 1-sun illumination with Voc of 0.534 V. Determined p-doping concentration in pillars using 4 point probe technique.
		4.2	C. Chang-Hasnain (510) 642-431	Improve pillar forest devices	Standard Microfabrication Techniques	>15% efficiency	Physical Specimen, Document									X	X	X	X					10/02/13	10/01/14	01/02/14	02/01/15	N/A	N/A	9.6 % for self assembled pillars under 1-sun illumination. 9% for top-down etched pillars under 1-sun illumination. Developed an ITO contact with resistivity of 1.8E-4Ωcm2 and calculated contact resistance of 180Ω for nanopillars
Phase IV	1	1	C. Chang-Hasnain (510) 642-431	Increase IQE of pillars	MOCVD, Optical Spectroscopy	90% IQE	Document													X	X	X	X	10/02/14	12/31/15			N/A	N/A	Developed undercut eching process that results in low dark current of 10pA and 10,000 fold reduction of current leakage.
	2	2.1	C. Chang-Hasnain (510) 642-431	Site-controlled pillar forest growth	Lithography, MOCVD, SEM	fill ratio>20%	Document													X	X	X	X	10/02/14	07/31/15			N/A	N/A	Improved density of pillars. Reproducible regrowth was achieved.
	3	4.2	C. Chang-Hasnain (510) 642-431	Achieve program goal	Standard Microfabrication Techniques	>20% efficiency	Physical Specimen, Document													X	X	X	X	10/02/14	12/31/15			N/A	N/A	Work on ex-situ p-doping of pillars to impove eficiency of devices: achieved low diode forward resistance of 3-7 KΩ

Award Number: **DE-EE0005316**
Project Title: **Single-Crystalline InGaAs/InP Dense Micro-Pillar Forest on Poly-Silicon Substrates for Low-Cost High-Efficiency Solar Cells**
Recipient: **Unversity of California, Berkeley**
Primary Contact: **Constance Chang-Hasnain**

II. Project Spend Plan (for Entire Project Period)

Instructions:

1) Initial Spend Plan: Enter the initial Spend Plan for the entire project in Columns A and C (gray columns).
Once entered, these amounts will NOT be changed for the entire period of the award.
2) Reporting Period: Enter the reporting period in the PINK cell below.

3) Fill in **actual outlays** for **past** quarters in the columns B. and D (green cells). (should match SF269 or SF425 Financial Status Report)
4) Adjust **projected outlays** for **present and all future** quarters columns B and D (please highlight these cells in blue).

Reporting Period:	1/01/2015 - 3/31/2015

Calendar Quarter	Year	From	To	A. Federal Share Initial Plan	B. Federal Share Updated Actuals & Plan	Cumulative Federal Share	C. Recipient Share Initial Plan	D. Recipient Share Updated Actuals & Plan	Cumulative Recipient Share
Q3	2011	7/1/2011	9/30/2011	$0	$0.00	$0.00	$0.00	$0.00	$0.00
Q4	2011	10/1/2011	12/31/2011	$66,433	$0.00	$0.00	$0.00	$0.00	$0.00
Q1	2012	1/1/2012	3/31/2012	$79,554	$46,724	$46,724.26	$0.00	$0.00	$0.00
Q2	2012	4/1/2012	6/30/2012	$69,386	$92,499	$139,223.24	$0.00	$0.00	$0.00
Q3	2012	7/1/2012	9/30/2012	$159,626	$124,736	$263,959.33	$0.00	$0.00	$0.00
Q4	2012	10/1/2012	12/31/2012	$65,366	$76,895	$340,854.80	$0.00	$0.00	$0.00
Q1	2013	1/1/2013	3/31/2013	$78,951	$42,239	$383,093.75	$0.00	$0.00	$0.00
Q2	2013	4/1/2013	6/30/2013	$68,159	$69,297	$452,390.31	$0.00	$0.00	$0.00
Q3	2013	7/1/2013	9/30/2013	$162,523	$112,404	$564,793.95	$0.00	$0.00	$0.00
Q4	2013	10/1/2013	12/31/2013	$63,657.03	$164,459	$729,252.51	$0.00	$0.00	$0.00
Q1	2014	1/1/2014	3/31/2014	$78,183.19	$34,310	$763,562.76	$0.00	$0.00	$0.00
Q2	2014	4/1/2014	6/30/2014	$65,433.16	$72,222	$835,784.70	$0.00	$0.00	$0.00
Q3	2014	7/1/2014	9/30/2014	$167,726.63	$185,088	$1,020,872.62	$0.00	$0.00	$0.00
Q4	2014	10/1/2014	12/31/2014	$62,437.04	$127,942	$1,148,814.60	$0.00	$0.00	$0.00
Q1	2015	1/1/2015	3/31/2015	$77,567.58	$56,452	$1,205,266.52	$0.00	$0.00	$0.00
Q2	2015	4/1/2015	6/30/2015	$63,921.58	$98,244	$1,303,511.01	$0.00	$0.00	$0.00
Q3	2015	7/1/2015	9/30/2015	$171,073.80	$98,244	$1,401,755.51	$0.00	$0.00	$0.00
Q4	2015	10/1/2015	12/31/2015	$0.00	$98,244	$1,500,000.00	$0.00	$0.00	$0.00
Q1	2016	1/1/2016	3/31/2016	$0.00	$0.00	$1,500,000.00	$0.00	$0.00	$0.00
Q2	2016	4/1/2016	6/30/2016	$0.00	$0.00	$1,500,000.00	$0.00	$0.00	$0.00
Totals				**$1,500,000.00**	**$1,500,000.00**	$1,500,000.00	**$0.00**	**$0.00**	$0.00

Updated Federal Spend Plan matches the baseline.

Updated Recipient Spend Plan matches the baseline.

Award Number: **DE-EE0005316**

Project Title: **Single-Crystalline InGaAs/InP Dense Micro-Pillar Forest on Poly-Silicon Substrates for Low-Cost High-Efficiency Solar Cells**

Recipient: **Unversity of California, Berkeley**

Primary Contact: **Constance Chang-Hasnain**

III. Spending Summary for SF 424A Budget Forms

Object Class Categories	Approved Budget ($)	Project Expenditures ($)	
Per SF 424a		This Reporting Period	Cumulative to Date
a. Personnel	$616,209	$31,705.26	$394,692.13
b. Fringe Benefits	$196,778	$13,294.46	$127,394.33
c. Travel	$43,008	$2,823.00	$20,218.58
d. Equipment		$2,570.60	$79,717.88
e. Supplies	$75,479	-$9,886.78	$208,636.76
f. Contractual			
g. Construction			
h. Other	$95,004	$146.00	$511.00
i. Total Direct Charges (sum of a to h)	$1,026,478	$40,652.54	$831,170.68
j. Indirect Charges	$473,522	$15,799.38	$374,095.84
k. Totals (sum of i and j)	**$1,500,000**	**$56,451.92**	**$1,205,266.52**
DOE Share	$1,500,000		
Cost Share	$0		
Calculated Cost Share Percentage	0.0%		

Award Number:
Project Title:
Recipient:
Primary Contact:

IV. Project Partners

Subrecipients / Project Participants	Cost Share Planned ($)	Cost Share Actual ($)	Location of Work
Subrecipient 1			
Subrecipient 2			
Subrecipient 3			
Subrecipient 4			
Subrecipient 5			
Subrecipient 6			
Subrecipient 7			
Subrecipient 8			
Subrecipient 9			
Subrecipient 10			
Other			

Contract ID of other Federally-funded projects on which you are currently an awardee or sub-awardee	
Contract ID	Awardee or Sub?

Award Number: DE-EE0005316
Project Title: Single-Crystalline InGaAs/InP Dense Micro-Pillar Forest on Poly-Silicon Substrates for Low-Cost High-Efficiency Solar Cells
Recipient: University of California, Berkeley
Primary Contact: Constance Chang-Hasnain

V. Accomplishments

A. Journal Articles

Full Author List	Article Title	Journal Name	Volume Number	No#	pp.	Year	URL
F. Ren, K.W. Ng, K. Li, H. Sun, and Connie J. Chang-Hasnain	High-quality InP nanoneedles grown on silicon	Applied Physics Letters	102		12115	2013	http://link.aip.org/link/doi/10.1063/1.4775377
K. W. Ng, T.-T. D. Tran, W. S. Ko, R. Chen, F. Lu, and C. J. Chang-Hasnain	Single Crystalline InGaAs Nanopillar Grown on Polysilicon with Dimensions beyond the Substrate Grain Size Limit	Nano letters	13		5931−5937	2013	http://pubs.acs.org/doi/abs/10.1021/nl403555z
K. Li, H. Sun, F. Ren, K. W. Ng, T.-T. D. Tran, R. Chen, and C. J. Chang-Hasnain	Tailoring the Optical Characteristics of Microsized InP Nanoneedles Directly Grown on Silicon	Nano letters	14		183−190	2014	http://pubs.acs.org/doi/abs/10.1021/nl403712f
R. Chen, K. W. Ng, W. S. Ko, D. Parekh, F. Lu, T.-T. D. Tran, K. Li, and C. J. Chang-Hasnain	Nanophotonic integrated circuits from nanoresonators grown on silicon	Nature Communications	5		4325	2014	http://www.nature.com/ncomms/2014/140707/ncomms5325/full/ncomms5325.html
H. Sun, F. ren, K. W. Ng, T.-T. D. Tran, K. Li, and C. J. Chang-Hasnain	Nanopillar Lasers Directly Grown on Silicon with Heterostructure Surface Passivation	ACS Nano	8	7	6833	2014	http://pubs.acs.org/doi/pdf/10.1021/nn501481u
T.-T. D. Tran, H. Sun, K. W. Ng, F. Ren, F. Lu, E. Yablonovitch, and, C. J. Chang-Hasnain	High brightness InP micropillars grown on silicon with Fermi level splitting larger than 1 eV	Nano Letters	14	6	3235	2014	http://pubs.acs.org/doi/abs/10.1021/nl500621j
K. W. Ng, W. So. Ko, F. Lu, and C. J. Chang-Hasnain	Metastable Growth of Pure Wurtzite InGaAs Microstructures	Nano Letters	14	8	4757	2014	http://pubs.acs.org/doi/abs/10.1021/nl501887f

B. Books, Book Chapters, Edited Volumes

Full Author List	Title	Edition	Volume Number	Publisher	# pages	Year	ISBN

C. Conference Publications

Full Author List	Article Title	Paper Number	Conference Proceedings Title or Conference Name	Conference Location	Dates	Volume	pp.	CD Rom Volume	ISBN

Conference Presentations

Full Author List	Paper Title	Paper No	Presented in the Season/Symposium Name at Conference Name	Conference Location	Dates
H. Sun, T. Tran, F. Ren, K. W. Ng, E. Yablonovitch, and C. J. Chang-Hasnain	Contactless I-V measurements on InP Micropillars grown in Silicon		International Nano-Optoelectronics Workshop (2012)	Berkeley and Palo Alto, CA	August 7-15, 2012
K. Li, F. Ren, R. Chen, T. Tran, K. W. Ng, and C. J. Chang-Hasnain	Characteristics of InP nanoneedles grown on silicon by low-temperature MOCVD	Tu-1D.3	IEEE 24th International Conference on Indium Phosphide and Related Materials (IPRM2012)	Santa Barbara, CA	August 27-30, 2012
H. Sun, T. Tran, F. Ren, K.W. Ng, E. Yablonovitch, C. J. Chang-Hasnain	High bandgap lattice-mismatched InGaP micropillars grown on Silicon	FF1.02	MRS Spring Meeting 2013	San Francisco, CA	April 1-5, 2013
T. Tran, H. Sun, F. Ren, K. W. Ng, K. Li, F. Lu, E. Yablonovitch, and C. J. Chang-Hasnain	Contactless I-V Measurements on InP Micropillars with Fermi-level Splits > 0.9V under 1 Sun	FF2.09	MRS Spring Meeting 2013	San Francisco, CA	April 1-5, 2013
T. Tran, H. Sun, F. Ren, K. W. Ng, K. Li, F. Lu, E. Yablonovitch, and C. J. Chang-Hasnain	High Brightness InP Micropillars Grown on Silicon with Fermi-level Splits Larger than 1 eV		39th IEEE Photovoltaic Specialists Conference	Tampa Bay, Florida	June 16-21, 2013

D	K. Li, T. Tran, K. W. Ng, H. Sun, F. L. Lu, and C. J. Chang-Hasnain	Single crystalline InP nanopillar grown on silicon with very low surface recombination velocity	Z9	55th Electronic Materials Conference (EMC2013)	South Bend, Indiana	June 26-28, 2013
	H. Sun, F. Ren, T.-T. D. Tran, K. W. Ng, K. Li and C. J. Chang-Hasnain	High Quality InGaP Micropillars Directly Grown on Silicon	WA1.2	IEEE summer topicals	Waikoloa, HI	July 8-10, 2013
	K. Li, T. Tran, K. W. Ng, H. Sun, F. L. Lu, and C. J. Chang-Hasnain	Single crystalline InP nanopillar grown on silicon with very low surface recombination velocity	SS9.04	Materials Research Society (MRS2013) Fall Meeting	Boston, MA	December 1-6, 2013
	I. Bhattacharya, T. Tran, H. Sun, K. W. Ng, F. Lu, E. Yablonovitch, C. J. Chang-Hasnain	Variability study of InP micropillars grown on a Si substrate towards ensemble solar cell devices		International Nano-Optoelectronics Workshop (2012)	Cargese, Corsica, France	August 19-30, 2013
	W. S. Ko, T. Tran, I. Bhattacharya, K. W. Ng, H. Sun, and C. J. Chang-Hasnain	Omnidirectional, high effiency single InP nanowire solar cell	Tu-A1-2	ISCS–Solar, CSW 2014	Montpellier, France	May 11-15, 2014
	H. Sun, K. W. Ng, F. Ren, T. Tran, K. Li and C. J. Chang-Hasnain	First Observation of Ordering from InGaP Microlasers in Wurtzite Phase	Mo-A2-1	IPRM-Epitaxy and Nanostructures 1, CSW 2014	Montpellier, France	May 11-15, 2014
	W. S. Ko, I. Bhattacharya, T. Tran, K. W. Ng, and C. J. Chang-Hasnain	InP nanowire avalanche photodiode and bipolar junction phototransistor integrated on silicon substrate	Mo-B1-2	IPRM–Photonic Integration 1, CSW 2014	Montpellier, France	May 11-15, 2014
	H. Sun, F. Ren, T. D. Tran, K. W. Ng, K. Li, W. Ko, I. Bhattacharya, C. J. Chang-Hasnain	High Voc Solar Absorbers for High Efficiency, Spectral Splitting Solar Cells	9	Bay Area Photovoltaic Consortium (BAPVC), BI-annual meeting 2014	Clark Kerr Conference Center University of California, Berkeley	6-7 October 2014

E	**Awarded Patents**			
	Full Inventor List	**Patent Title**	**Year**	**Patent Number**

F	**Students graduated and their Current Positions**				
	Name	**MS/Ph.D**	**Started (Fall/Spring/Summer 20YY)**	**Graduated (Defense Date)**	**Current Position and Affiliation**
	Wai Son Ko	Ph.D	Summer 2008	Jul-14	Infinera, Sunnyvale, CA, USA / Test
	Thai-Truong D. Tran	Ph.D	Summer 2008	graduated in December 2013, finished work as a postdoc researched on 08/31/2014	Boston Consulting Group, Germany / Consultant

G	**Major Honors and Awards**		
	Award	**Sponsor**	**Date of Award**

H	**Private Funding (e.g. Venture Capital, Private Equity, etc.) Awarded Following this Award**		
	Private Capital Partner	**Amount of Funding**	**Months since DOE Award announcement**

I	**Other Accomplishments**		